Applied Physics B (2019) 125:173
https://doi.org/10.1007/s00340-019-7288-7

Applied Physics B
Lasers and Optics

Lasing characteristics of heavily doped single-crystal Fe:ZnSe

V. A. Antonov[2] · A. A. Davydov[1] · K. N. Firsov[2,3] · E. M. Gavrishchuk[4,5] · I. G. Kononov[2] · S. V. Kurashkin[4] · S. V. Podlesnykh[2] · N. A. Raspopov[6] · N. V. Zhavoronkov[1]

Received: 20 June 2019 / Accepted: 17 August 2019 / Published online: 24 August 2019

Abstract
Characteristics of a Fe:ZnSe laser are studied at room temperature. The laser active elements are heavily doped single crystals with the Fe^{2+} ion concentration $n = 0.64 \times 10^{19} - 5.7 \times 10^{19}\text{cm}^{-3}$, grown from melt by the Bridgman method. The generated energy of 870 mJ is obtained at the total efficiencies with respect to the absorbed and incident energies $\eta_{\text{abs}} = 43\%$ and $\eta_{\text{inc}} \approx 35\%$, respectively. The laser slope efficiency with respect to the absorbed energy is $\eta_{\text{slope}} \approx 50\%$. In a heavily doped active element with the Fe^{2+} concentration $n = 5.7 \times 10^{19}\text{cm}^{-3}$, in which the medium excitation depth is just a part of the total element dimension along the optical axis (the element is completely non-transparent for the pumping radiation), the radiation spectrum of the Fe:ZnSe laser shifts to the long-wavelength range by more than 300 nm as compared to spectra of the laser on crystals excited along the whole element length. It is shown that Fe:ZnSe lasers on heavily doped single-crystal elements can be efficiently excited by a radiation of a Cr:ZnSe laser without tuning the spectrum of the latter to the longer wavelength range.

Keywords Fe:ZnSe laser · HF laser · Single crystal · Room temperature · Zinc chalcogenides · Bridgman method · Cr:ZnSe laser

1 Introduction

In the recent 20 years, lasers on Fe:ZnSe crystals have been actively studied in numerous groups [1–30]. Recently, improved technologies for producing active elements [22, 23, 27] substantially increased the efficiency of a Fe:ZnSe laser and lasers on crystals of other chalcogenides doped with transition metal ions. In first papers (see, for example, [2–6, 10]), the value of slope efficiency of a Fe:ZnSe laser with respect to the absorbed energy η_{slope} did not exceed 40% at room temperature of an active element. Presently, the efficiencies reached on polycrystalline elements with large transversal dimensions doped in the process of hot isostatic pressing (HIP) [22, 31, 32] and single-crystal doped in the growing process [30] are $\eta_{\text{slope}} = 53\%$ [22] and $\eta_{\text{slope}} = 45\%$ [15, 20], respectively.

A low Fe^{2+} concentration is a specific feature of high-quality single-crystal active elements grown on a single-crystal seed from vapour phase by chemical transport in hydrogen [3, 7, 12, 30] and doped with iron in the growing process. In view of this fact, longer crystals or sufficiently complicated pumping schemes are used [33], which is not always convenient. For example, the concentration of Fe^{2+} in an active element of the Fe:ZnSe laser on which the highest radiation energy has been presently obtained for single crystals at room temperature [15, 20] was $\sim 1.5 \times 10^{18}$ cm^{-3} at the active element length of 15 mm. The main incentive to use long single crystals with low Fe^{2+} concentration as active elements in [15, 20] was the possibility to reduce the

✉ K. N. Firsov
k_firsov@rambler.ru

[1] Research Institute of Material Science and Technology JSC RIMST, RIMST, Georgievskiy prospect, 5, Building 2, 124460 Zelenograd, Moscow, Russia

[2] A.M. Prokhorov General Physics Institute of RAS, 38 Vavilov Str., 119991 Moscows, Russia

[3] National Research Nuclear University MEPhI, Kashirskoye shosse 31, 115409 Moscow, Russia

[4] G.G. Devyatykh Institute of Chemistry of High-Purity Substances of RAS, 49 Troponina St., 603950 Nizhny Novgorod, Russia

[5] N.I. Lobachevski Nizhny Novgorod State University, 23 Gagarin Avenue, 603950 Nizhny Novgorod, Russia

[6] P N Lebedev Physical Institute of RAS, 53 Leninsky pr., 119991 Moscow, Russia

gain of excited medium to worsen the development conditions for parasitic transversal oscillation at large pumping spot dimensions. Just the development of parasitic oscillation was the main factor limiting the generation energy of a Fe:ZnSe laser on polycrystals with a high Fe^{2+} concentration in the near-surface layer of elements excited by a high-power HF laser at room temperature [10, 18]. However, further investigations revealed the possibility to suppress parasitic oscillation by simply increasing transversal dimensions of a polycrystalline active element even at sufficiently high Fe^{2+} concentrations in both ZnSe and ZnS hosts [22, 34]. A similar result is obtained using active elements with several inner doped layers [17, 25] or elements with an internal doped layer in the form of a spherical segment [29].

Obviously, in the case of single-crystal Fe:ZnSe active elements with a high concentration of bivalent iron (heavily doped crystals), the problem of parasitic oscillation at large pumping spot dimensions can be solved by simply increasing the sample transversal dimensions. From general consideration, we may also expect that introducing the doping component into the host at a higher than conventional concentration may change the pumping energy threshold, efficiency, and generation spectrum of the laser. Nevertheless, we failed to find works focused on studying characteristics of Fe:ZnSe lasers with heavily doped single crystals used as active elements. Thus, the aim of the present work is to perform such undoubtedly interesting investigations using heavily doped single crystals grown by modern technologies.

2 Fe:ZnSe single-crystal sample fabrication technology

The problem of fabricating zinc selenide crystals doped with transition metals such as chromium or iron has several solutions. First, it is introducing a doping component in the process of crystal growing. In the case of growing from melt (for example, by the Bridgman method, or its modifications), the problem is solved sufficiently simply by introducing a required component in an appropriate form to the initial blend. Conventionally, components well mix in the melt, which provides a homogeneously doped crystal with a prescribed admixture composition. The method is rather efficient, a ZnSe crystal of weight 0.5 kg and more grows for 60–70 h. There are no principal limitations on crystal transversal dimensions. A drawback of the crystal growth from melt, which is specific for A2B6 compounds, is the tendency of grown object to form blocks and twins. Mostly perfect single crystals of A2B6 compounds and their triple solid solutions are fabricated by the Davydov–Markov method from vapour phase [35]. However, with this method, it is difficult to dope crystals with transition metals, which have a low vapour pressure. It is also difficult to obtain homogeneous doping. Efficiency of the method is low (a crystal of weight 150–200 g grows for 180–250 h) and there are serious limitations on crystal dimensions. The third method for producing zinc selenide crystals doped with transition metal admixtures is diffusion. This method provides a high dopant concentration in a near-surface region, however, with a high gradient of concentration along the sample depth.

In the present work, we studied two single-crystal active elements Fe:ZnSe with the Fe^{2+} concentrations differing by almost an order of magnitude. The crystals were grown by the vertical Bridgman method in a graphite container at an argon pressure of 30 atm. The initial high-purity (99.9999%) polycrystalline ZnSe was synthesized by the chemical vapor deposition. Iron admixture was added to the initial load in the form of FeSe. The rate of crystal growth was 1–3 mm h^{-1}. In a transversal cross section, the first crystal (sample 1) had a shape of a segment with a height of 25 mm. The sample thickness was 5 mm. It was cut from a boule of diameter 50 mm and length 80 mm. The concentration of Fe^{2+} ions in sample 1, determined from a transmission spectrum and absorption cross-sectional data [27], was $n = 6.4 \times 10^{18}$ cm^{-3}. The second active element (sample 2) had the form of disk with a diameter of 50 mm and thickness of 1.8 mm; the Fe^{2+} concentration was $n = 5.7 \times 10^{19}$ cm^{-3}. Transmission spectra of the single crystals studied are presented in Fig. 1.

The luminescence lifetimes of Fe^{2+} in samples 1 and 2 are 320 and 250 ns, respectively. The method of determining the luminescence lifetime is similar to that used in [14]. The reduction of the luminescence lifetime down to 250 ns in the case of heavy doping is not critical because the pumping pulse duration in the experiments described below was substantially shorter than this value. For measuring the luminescence lifetime, the crystals were excited by a pulsed laser at the wavelength $\lambda = 2.94$ µm. Signals of Fe^{2+} luminescence were recorded by a photodetector PD47NB ("Ioffe LED,

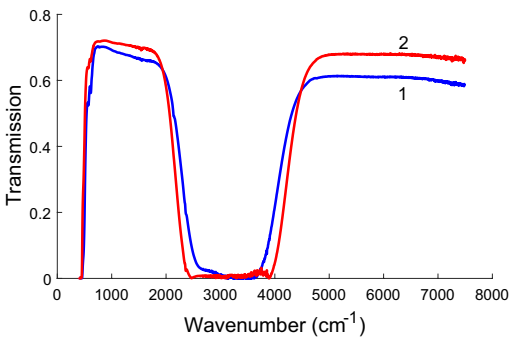

Fig. 1 Transmission spectra of single-crystal sample Fe:ZnSe: (1)—sample 1, $n = 6.4 \times 10^{18}$ cm^{-3}; (2)—sample 2, $n = 5.7 \times 10^{19}$ cm^{-3}

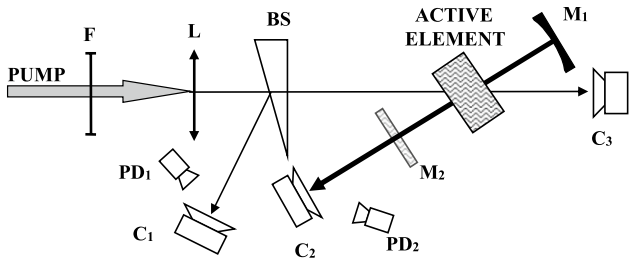

Fig. 2 Scheme of experiment: *M1, M2* cavity mirrors, *F* optical filter, *L* spherical lens, *BS* beam splitter, *C1, C2, C3* calorimeters, *PD1, PD2* photodetectors

Ltd") with an amplifier. The time resolution of the recording system was 100 ns.

3 Experimental setup for laser experiments

The method used for studying lasing characteristics of single-crystal active elements did not differ much from those described earlier (see, for example, [21, 22]). For easy understanding of further consideration, an optical schematic diagram of experiments is presented in Fig. 2. A non-chain HF laser was a pumping source for the crystals [15, 22]. The cavity of a Fe:ZnSe laser of length 130 mm was formed by a concave spherical mirror with gold coating M1 having the radius of curvature 0.5 m and plane outcoupling mirror M2 with the reflection coefficient of 40% in the spectral range of 4.2–5 μm. Energies of the pumping radiation incident onto the crystal, radiation passed through it, and generation of the Fe:ZnSe laser were measured by calorimeters C1÷C3 ("Molectron"). The radiation from HF laser was attenuated by a set of light filters F and focused on the surface of active element by lens L. By moving the lens, we varied the size of a pumping beam on the sample surface. The angle of pumping beam incidence to the crystal surface was 10°.

Profiles of laser radiation pulses were recorded by photodetectors PD_1 and PD_2 ("Vigo-system Ltd") with the time resolution of ≈ 1 ns. A high sensitivity of photodetectors provided recording the radiation scattered by calorimeter input areas. Spectra of Fe:ZnSe laser radiation were recorded by a MS 2004 ("SOLAR TII") monochromator with a linear array of pyroelectric photodetectors HPL-256-500 (HEIMANN Sensor) at output (is not shown in Fig. 2).

4 Results and discussion

From Fig. 1 it follows that at low energy densities, both the crystals are not transparent at the wavelengths of HF laser pumping generation $\lambda = 2.6 - 3.1$ μm. In the conditions of Fe:ZnSe laser generation, at the pumping energy density exceeding 1 J cm^{-2}, the transmission of sample 1 was 4%. Sample 2 remained non-transparent for the pumping radiation even in the generation conditions. Dependencies of generation energy of a Fe:ZnSe laser on the HF-laser energy absorbed in the crystal are shown in Fig. 3 for various diameters of the pumping spot on the surface of sample 1. From Fig. 3, one can see that the slope efficiency of the Fe:ZnSe laser on heavily doped single crystals at a sufficiently large pumping spot diameter $d = 10$ mm is $\eta_{slope} \approx 50\%$, which is greater than the value obtained earlier $\eta_{slope} \approx 45\%$ on the sample with the Fe^{2+} concentration $n = 1.5 \times 10^{18}$ cm^{-3} [15, 20]. The higher slope efficiency at greater pumping spot dimensions testifies a high quality of the active element under study. Up to now, the value of η_{slope} with Fe:ZnSe single crystals, grown by the Bridgman method did not exceed $\eta_{slope} = 42\%$ [16]. The maximum generation energy reached with sample 1 was 870 mJ at the total efficiencies with respect to the absorbed and incident energies $\eta_{abs} = 43\%$ and $\eta_{inc} \approx 35\%$, correspondingly. The laser total efficiency with respect to the incident energy obtained in the present work is also above that reported earlier in [15, 20] with weakly doped single crystal ($\eta_{inc} \approx 25\%$). In particular, it is a consequence of actually total absorption of the pumping energy in the active element (without AR coating) in the considered case (except for the reflection losses on the input face). With sample 1, the generation energy was limited by the transversal parasitic oscillation developing at pumping spot diameters exceeding 11 mm due to a relatively small one of the transversal dimensions of the active element (the segment height). Undoubtedly, this limitation can be removed similar to the case of polycrystalline active elements [22] by increasing transversal dimensions of the

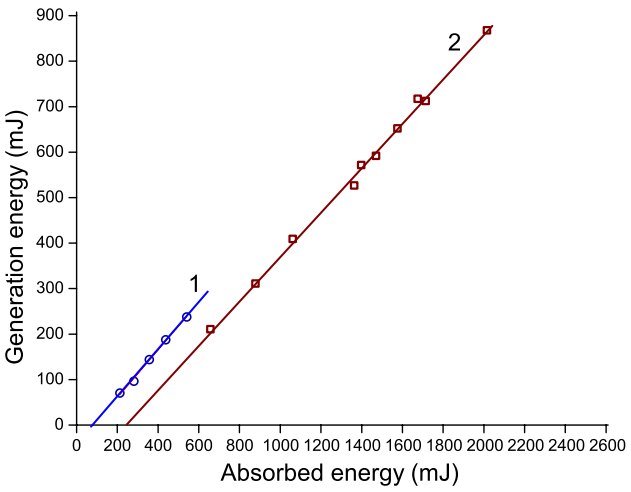

Fig. 3 Generation energy of the Fe:ZnSe laser versus the absorbed energy at the pumping spot diameter $d = 5$ mm (1) and $d = 10$ mm (2). Sample 1, $n = 6.4 \times 10^{18}$ cm^{-3}

sample, for example, using a disk of diameter 50 mm rather than a segment cut from it. There are no principal limitations on fabricating crystals of diameter 50 mm and greater by the technology employed.

As mentioned, the second sample with the Fe^{2+} concentration $n = 5.7 \times 10^{19}$ cm^{-3} is completely non-transparent for the pumping radiation even in the conditions of Fe:ZnSe laser generation. Simple estimates show that the depth of pumping radiation penetration into the crystal is at most 200 µm, that is, a greater part of the crystal is not excited in the direction of the optical axis, forming a kind of an optical filter because the unexcited Fe:ZnSe noticeably absorbs in the spectral range of 4–5 µm [27]. The absorption at the generation wavelengths in an unexcited medium just allows one to avoid a transversal parasitic generation at small diameters of the pumping spot by increasing transversal dimensions of the active element [22]. Dependencies of the generation energy of the Fe:ZnSe laser on the absorbed HF laser energy are shown in Fig. 4 for various diameters of the pumping spot on sample 2. From Fig. 4, one can see that despite the fact that the active element is totally opaque for the pumping radiation, the slope efficiency of the Fe:ZnSe laser on sample 2 with respect to the absorbed energy is sufficiently large $\eta_{slope} = 37\%$. The maximum generation energy is 245 mJ at the total efficiency with respect to the absorbed energy $\eta_{abs} \approx 22\%$. However, already at a pumping spot diameter exceeding $d = 7.4$ mm, a parasitic oscillation is revealed (the laser slope efficiency falls), whereas the transversal crystal dimensions are much greater than 20 mm (the diameter of 20 mm). At such a value, the spot diameter $d = 7.4$ mm on polycrystalline samples doped by the diffusion method from both crystal sides was the limiting dimension, above which the output characteristics of a Fe:ZnSe laser sharply fall due to the developing parasitic oscillation [18]. We may assume that in the case considered in the present work, a parasitic oscillation at large pumping spot dimensions may develop without the feedback formed by the radiation scattered from sample edges (superluminescence), because all the pumping energy is absorbed in a very thin layer near the surface, where a high gain is attained. Such a regime was realized in [4, 8] under the transversal pumping of Fe:ZnSe single crystals doped with iron by the diffusion method. A thickness of the doped layer in those active elements was ~ 100 µm.

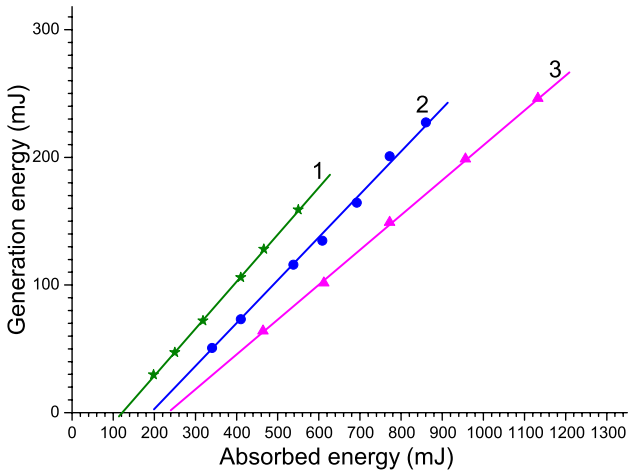

Fig. 4 Generation energy of the Fe:ZnSe laser versus the absorbed energy at the pumping spot diameter $d = 6$ mm (1), $d = 7.4$ mm (2), and $d = 8.1$ mm (3). Sample 2, $n = 5.7 \times 10^{19}$ cm^{-3}

Oscillograms of the pumping pulse and generation of Fe:ZnSe lasers obtained on samples 1 and 2 at close values of energy absorbed in the crystals are presented in Fig. 5. From Fig. 5, one can see that generation pulses of Fe:ZnSe lasers on samples 1 and 2 only differ in insignificant details (the generation pulse of laser on sample 2 is slightly shorter than on sample 1) despite the Fe:ZnSe unexcited layer present in sample 2, which noticeably absorbs radiation in the spectral range of 4–5 µm (see Fig. 1). We may assume that when generation develops in the laser on sample 2, the unexcited layer "bleaches". To illustrate this fact we have recorded the transmission of sample 2 versus the energy density of Fe:ZnSe laser incident on a surface of the sample. The pumping source in this case was the Fe:ZnSe laser on sample 1 excited by an HF laser. This dependence is shown in Fig. 6. For comparison, in the same figure we present the absorption curve for a high-quality polycrystalline Fe:ZnSe sample studied earlier [22]. In Fig. 6 one can see that the polycrystalline sample actually totally ""bleaches" already at the density of energy incident onto the surface $w_{in} = 0.3–0.4$J cm^{-2}. The initial transmission of this sample at low energy densities was ≈ 6%. The single-crystal sample also "bleaches"; however, its transmission at our maximal experimental energy density $w_{in} = 1.5$J cm^{-2} is only 55% in contrast to 66% in the case of polycrystalline sample.

Generation spectra of Fe:ZnSe lasers on samples 1 and 2 are presented in Fig. 7. From Fig. 7, one can see that the spectrum of laser on sample 1 insignificantly differs from those obtained earlier (see, for example, [11, 21]) for Fe:ZnSe lasers on polycrystalline active elements. The spectrum of the laser on heavily doped crystal (sample 2) is

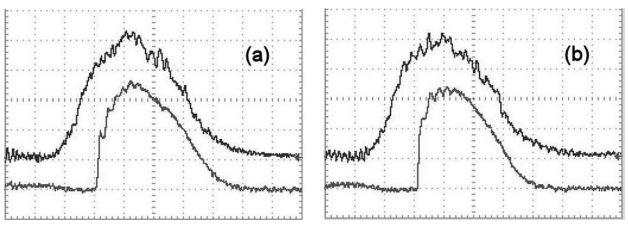

Fig. 5 Oscillograms of the pumping pulse (top ray) and Fe:ZnSe-laser generation (bottom ray) recorded for samples 1 (**a**) and 2 (**b**). The timescale is 50 ns/div

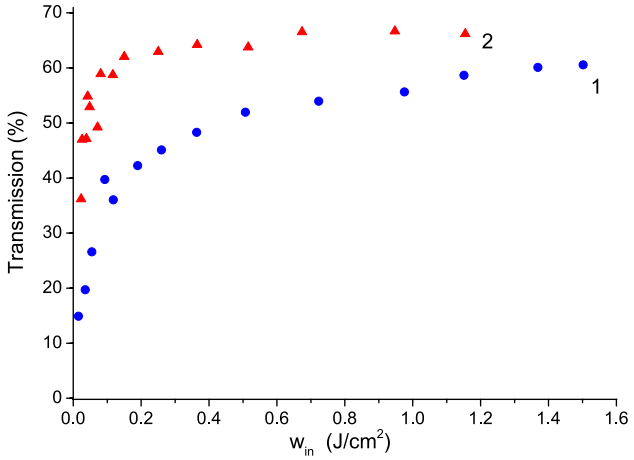

Fig. 6 Transmission of sample 2 (1) and polycrystalline sample (2) versus the radiation energy density of a Fe:ZnSe laser w_{in} on the surface

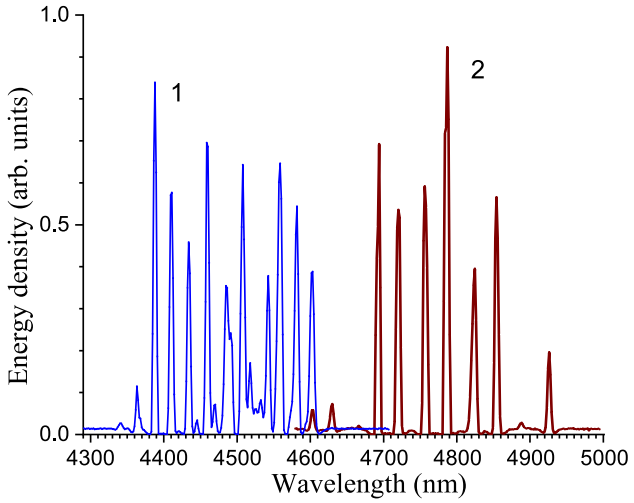

Fig. 7 Generation spectra of Fe:ZnSe laser: 1—sample 1, $n = 0.64 \times 10^{19}$cm^{-3}; 2—sample 2, $n = 5.7 \times 10^{19}$ cm^{-3}

shifted to the long-wavelength range by more than 300 nm relative to the spectrum obtained with sample 1. Obviously, the spectral shift is related to the dependence of absorption cross section on wavelength in the unexcited zone of sample 1. In the spectral range of 4.3–5 µm, the absorption falls at greater wavelengths [27]. Note that the shift of generation spectrum to longer wavelengths by ≈ 300 nm was observed by authors of [16] when the active element on Fe:ZnSe crystal was replaced with that on Fe:ZnMgSe. However, such a replacement resulted in a more than fourfold reduction of the laser slope efficiency with the corresponding fall in the output energy. In the present work, the slope efficiency reduced by only ≈ 25%. Note also that the spectrum shift to the long-wavelength range observed in [16] and in the present work can be easily obtained on Fe:ZnSe crystals with ordinary characteristics by means of spectral profiling the reflection coefficient of the outcoupling mirror.

Consider one more possible application of heavily doped single crystals with the characteristics of sample 2 (or crystals with less concentration of iron ions but greater length). Mirov et al. reported [35] the employment of a well-developed Cr:ZnSe laser for pumping a Fe:ZnSe laser. In that case, the spectral tuning of the Cr:ZnSe laser to the longer wavelength range was needed for matching its emission spectrum with the absorption band of bivalent iron in a Fe:ZnSe crystal, which reduced the efficiency of the laser system as a whole. A typical generation spectrum of a Cr:ZnSe laser with non-selective cavity described in [37] is presented in Fig. 8 along with the transmission spectrum of sample 2 plotted using data from Fig. 1 in the same spectral range. One can see that the Cr:ZnSe laser is well suited for pumping the Fe:ZnSe laser on the active element with sample 2. A better matching between the generation spectrum of the Cr:ZnSe laser and the crystal absorption spectrum may be obtained by slightly increasing the sample thickness. Note also that an increase of Fe^{2+} concentration in the sample easily realisable in the technology considered is a simpler and more efficient method for matching the absorption and pumping spectra as compared to, for example, doping the solid solution $ZnS_xSe_{(1-x)}$ with iron ions considered in [26].

5 Conclusion

Thus, in the present work we investigate generation and spectral characteristics of a Fe:ZnSe laser on heavily doped single crystals, in which the concentration of Fe^{2+} reached the values $n = 5.7 \times 10^{19}$cm^{-3}. The generation energy

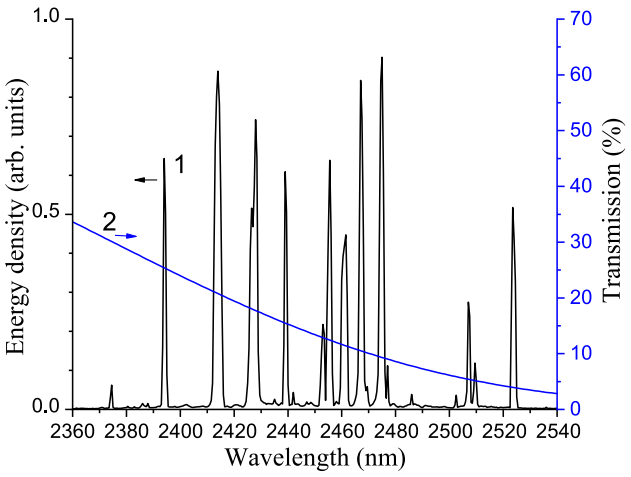

Fig. 8 Generation spectrum of Cr:ZnSe laser (1) and transmission spectrum of heavily doped single crystal (sample 2) (2)

of 870 mJ has been obtained at the total efficiencies with respect to the absorbed and incident energies $\eta_{abs} = 43\%$ and $\eta_{inc} \approx 35\%$, respectively. Possibilities for further energy increase were limited by the parasitic oscillation, which developed at large pumping spot dimensions. This limitation can be removed by increasing the transversal dimensions of active elements, which can be easily done with the Bridgman technology of crystal growing from melt. Possibilities of using heavily doped crystals for shifting the generation spectrum of a Fe:ZnSe laser to a long-wavelength range and for fabricating Fe:ZnSe lasers pumped by the radiation of a Ce:ZnSe laser without additional spectrum correction are demonstrated. Results obtained testify a high quality of the Fe:ZnSe single crystals grown by the Bridgman method.

Acknowledgements This work was supported by the Russian Science Foundation, Grant no. 19-13-00205 (development of the technique for creating Fe:ZnSe samples and preparation of active elements for experiments) and by the Russian Foundation for Basic Research, project no. 18-08-00793 (study of laser characteristics).

References

1. J.J. Adams, C. Bibeau, R.H. Page, D.M. Krol, L.H. Furu, S.A. Payne, Opt. Lett. **24**(23), 1720–1722 (1999)
2. J. Kernal, V.V. Fedorov, A. Gallian, S.B. Mirov, V.V. Badikov, Opt. Express **13**, 10608–10612 (2005)
3. V.A. Akimov, A.A. Voronov, V.I. Kozlovsky, Y.V. Korostelin, A.I. Landman, Y.P. Podmarkov, M.P. Frolov, Quantum Electron. **36**(4), 299–302 (2006)
4. N.N. Il'ichev, V.P. Danilov, V.P. Kalinushkin, M.I. Studenikin, P.V. Shapkin, A.S. Nasibov, Quantum Electron. **38**(2), 95–96 (2008)
5. M.E. Doroshenko, H. Jelinkova, P. Koranda, J. Sulc, T.T. Basiev, V.V. Osiko, V.K. Komar, A.S. Gerasimenko, V.M. Puzikov, V.V. Badikov, D.V. Badikov, Laser Phys. Lett. **7**(1), 38–45 (2010)
6. N.S. Myoung, D.V. Martyshkin, V.V. Fedorov, S.B. Mirov, Opt. Lett. **36**(1), 94–96 (2011)
7. M.P. Frolov, Y.V. Korostelin, V.I. Kozlovsky, V.V. Mislavskii, Y.P. Podmarkov, S.A. Savinova, Y.K. Skasyrsky, Laser Phys. Lett. **10**, 125001 (2013)
8. S.D. Velikanov, V.P. Danilov, N.G. Zakharov, N.N. Il'ichev, SYu. Kazantsev, V.P. Kalinushkin, I.G. Kononov, A.S. Nasibov, M.I. Studenikin, P.P. Pashinin, K.N. Firsov, P.V. Shapkin, V.V. Shchurov, Quantum Electron. **44**(2), 141–145 (2014)
9. E.M. Gavrishchuk, SYu. Kazantsev, I.G. Kononov, S.A. Rodin, K.N. Firsov, Quantum Electron. **44**(6), 505–506 (2014)
10. K.N. Firsov, E.M. Gavrishchuk, SYu. Kazantsev, I.G. Kononov, S.A. Rodin, Laser Phys. Lett. **11**(8), 085001 (2014)
11. K.N. Firsov, E.M. Gavrishchuk, SYu. Kazantsev, I.G. Kononov, A.A. Maneshkin, G.M. Mishchenko, S.M. Nefedov, S.A. Rodin, S.D. Velikanov, I.M. Yutkin, N.A. Zaretsky, E.A. Zotov, Laser Phys. Lett. **11**(12), 125004 (2014)
12. S.D. Velikanov, N.A. Zaretskii, E.A. Zotov, V.I. Kozlovskii, Y.V. Korostelin, O.N. Krokhin, A.A. Maneshkin, Y.P. Podmar'kov, S.A. Savinova, Y.K. Skasyrskii, M.P. Frolov, R.S. Chuvatkin, I.M. Yutkin, Quantum Electron. **45**, 1–7 (2015)
13. Jonathan W. Evans, Patrick A. Berry, Kenneth L. Schepler, Opt. Lett. **37**(23), 5021–5023 (2012)
14. N.S. Myoung, V.V. Fedorov, S.B. Mirov, L.E. Wenger, J. Lumin. **132**(3), 600–606 (2012)
15. K.N. Firsov, M.P. Frolov, E.M. Gavrishchuk, SYu. Kazantsev, I.G. Kononov, A.A. YuV Korostelin, S.D. Maneshkin, I.M. Velikanov, N.A. Yutkin, E.A.Zotov Zaretsky, Laser Phys. Lett. **13**(1), 015002 (2016)
16. H. Jelinkova, M.E. Doroshenko, M. Jelinek, J. Sulc, M. Nemec, V. Kubecek, Y.A. Zagoruiko, N.O. Kovalenko, A.S. Gerasimenko, V.M. Puzikov, V.K. Komar, Fe:ZnSe and Fe:ZnMgSe lasers pumped by Er:YSGG radiation. International Society for Optics and Photonics. In: Solid State Lasers XXIV: Technology and Devices **9342** 93421V
17. K.N. Firsov, E.M. Gavrishchuk, V.B. Ikonnikov, SYu. Kazantsev, I.G. Kononov, T.V. Kotereva, D.V. Savin, N.A. Timofeeva, Laser Phys. Lett. **13**(5), 055002 (2016)
18. E.M. Gavrishchuk, V.B. Ikonnikov, SYu. Kazantsev, I.G. Kononov, S.A. Rodin, D.V. Savin, N.A. Timofeeva, K.N. Firsov, Quantum Electron. **45**(9), 823–827 (2015)
19. S.B. Mirov, V. Fedorov, D. Martyshkin, I. Moskalev, M. Mirov, S. Vasilyev, Advanced Solid State Lasers Conference, Berlin Germany, (2015) AW4A.1
20. S.D. Velikanov, N.A. Zaretsky, E.A. Zotov, SYu. Kazantsev, I.G. Kononov, YuV Korostelin, A.A. Maneshkin, K.N. Firsov, M.P. Frolov, I.M. Yutkin, Quantum Electron. **46**, 11–12 (2016)
21. S.D. Velikanov, E.M. Gavrishchuk, N.A. Zaretsky, A.V. Zakhryapa, V.B. Ikonnikov, SYu. Kazantsev, I.G. Kononov, A.A. Maneshkin, D.A. Mashkovskii, E.V. Saltykov, K.N. Firsov, R.S. Chuvatkin, I.M. Yutkin, Quantum Electron. **47**, 303 (2017)
22. A.E. Dormidonov, K.N. Firsov, E.M. Gavrishchuk, V.B. Ikonnikov, SYu. Kazantsev, I.G. Kononov, T.V. Kotereva, D.V. Savin, N.A. Timofeeva, Appl. Phys. B **122**, 211 (2016)
23. V.I. Kozlovsky, Y.V. Korostelin, YuP Podmar'kov, Y.K. Skasyrsky, M.P. Frolov, Efficient 10-J pulsed Fe:ZnSe laser at 4100 nm. J. Phys. Conf. Ser. **740**, 012006 (2016)
24. R.I. Avetisov, S.S. Balabanov, K.N. Firsov, E.M. Gavrishchuk, A.A. Gladilin, V.B. Ikonnikov, V.P. Kalinushkin, SYu. Kazantsev, I.G. Kononov, M.P. Zykova, E.N. Mozhevitina, A.V. Khomyakov, D.V. Savin, N.A. Timofeeva, O.V. Uvarov, ICh. Avetissov, J. Cryst. Growth **491**, 36–41 (2018)
25. S.S. Balabanov, K.N. Firsov, E.M. Gavrishchuk, V.B. Ikonnikov, SYu. Kazantsev, I.G. Kononov, T.V. Kotereva, D.V. Savin, N.A. Timofeeva, Laser Phys. Lett. **15**, 045806 (2018)
26. K.N. Firsov, E.M. Gavrishchuk, V.B. Ikonnikov, SYu. Kazantsev, T.V. Kotereva, D.V. Savin, N.A. Timofeeva, Phys. Wave Phenom. **26**(1), 1–6 (2018)
27. S.B. Mirov, I.S. Moskalev, S. Vasilyev, V. Smolski, V.V. Fedorov, D. Martyshkin, J. Peppers, M. Mirov, A. Dergachev, V. Gapontsev, IEEE J. Sel. Top. Quantum Electron. **24**(5), 1–29 (2018)
28. V.V. Fedorov, S.B. Mirov, A. Gallian, D.V. Badikov, M.P. Frolov, YuV Korostelin, V.I. Kozlovsky, A.I. Landman, YuP Podmar'kov, V.A. Akimov, A.A. Voronov, IEEE J. Quantum Electron. **42**(9), 907–917 (2006)
29. S.S. Balabanov, K.N. Firsov, E.M. Gavrishchuk, V.B. Ikonnikov, I.G. Kononov, S.V. Kurashkin, S.V. Podlesnykh, D.V. Savin, A.A. Sirotkin, Laser Phys. Lett. **16**, 055004 (2019)
30. V.I. Kozlovsky, V.A. Akimov, M.P. Frolov, YuV Korostelin, A.I. Landman, V.P. Martovitsky, V.V. Mislavskii, YuP Podmar'kov, YaK Skasyrsky, A.A. Voronov, Phys. Status Sol. B **247**(6), 1553–1556 (2010)
31. E.M. Gavrishchuk, Inorg. Mater. **39**, 883–899 (2003)
32. E.M. Gavrishchuk, V.B. Ikonnikov, D.V. Savin, Inorg. Mater. **50**, 222–227 (2014)
33. A.A. Voronov, Generatsionnye i spektral'no-kineticheskie kharakteristiki lazera na kristalle Fe^{2+}:ZnSe (Emission and Spectral-Kinetic Characteristics of Laser on Fe^{2+}:ZnSe crystal). PhD thesis (2009) **(in Russian)**

34. K.N. Firsov, E.M. Gavrishchuk, V.B. Ikonnikov, SYu. Kazantsev, I.G. Kononov, S.A. Rodin, D.V. Savin, N.A. Timofeeva, Laser Phys. Lett. **13**(1), 015001 (2016)
35. S.B. Mirov, V.V. Fedorov, D.V. Martyshkin, I.S. Moskalev, M.S. Mirov, S.V. Vasilyev, IEEE J. Sel. Top. Quantum Electron. **21**, 1601719 (2015)
36. A.A. Davydov, V.N. Ermolov, S.V. Neustroev, L.P. Pavlova, Neorganicheskie Materialy **28**(1–6), 42–48 (1992). [in Russian]
37. S.V. Kurashkin, O.V. Martynova, D.V. Savin, E.M. Gavrishchuk, S.A. Rodin, A.P. Savikin, Laser Phys. Lett. **15**, 025002 (2018)